Highly insulating thermoplastic blends comprising a styrenic copolymer for direct-current power cable insulation

(article starts on next page)

国家电网
STATE GRID
中国电力科学研究院有限公司
CHINA ELECTRIC POWER RESEARCH INSTITUTE

IET The Institution of Engineering and Technology WILEY

ORIGINAL RESEARCH

Highly insulating thermoplastic blends comprising a styrenic copolymer for direct-current power cable insulation

Yingwei Ouyang[1] | Amir Masoud Pourrahimi[1] | Ida Östergren[1] |
Marcus Mellqvist[1] | Jakob Ånevall[1] | Azadeh Soroudi[1] | Anja Lund[1] |
Xiangdong Xu[2] | Thomas Gkourmpis[3] | Per-Ola Hagstrand[3] | Christian Müller[1]

[1]Department of Chemistry and Chemical Engineering, Chalmers University of Technology, Göteborg, Sweden

[2]Department of Electrical Engineering, Chalmers University of Technology, Göteborg, Sweden

[3]Innovation & Technology, Borealis AB, Stenungsund, Sweden

Correspondence

Per-Ola Hagstrand, Innovation & Technology, Borealis AB, 44486 Stenungsund, Sweden.
Email: per-ola.hagstrand@borealisgroup.com

Christian Müller, Department of Chemistry and Chemical Engineering, Chalmers University of Technology, 41296 Göteborg, Sweden.
Email: christian.muller@chalmers.se

Associate Editor: Xingyi Huang.

Funding information

Stiftelsen för Strategisk Forskning; Borealis AB

Abstract

The impact of the composition of blends comprising low-density polyethylene (LDPE), isotactic polypropylene (PP) and a styrenic copolymer additive on the thermomechanical properties as well as the direct-current (DC) electrical and thermal conductivity is investigated. The presence of 5 weight percent (wt%) of the styrenic copolymer strongly reduces the amount of PP that is needed to enhance the storage modulus above the melting temperature of LDPE from 40 to 24 wt%. At the same time, the copolymer improves the consistency of the thermomechanical properties of the resulting ternary blends. While both the DC electrical and thermal conductivity strongly decrease with PP content, the addition of the styrenic copolymer appears to have little influence on either property. Evidently, PP in combination with small amounts of a styrenic copolymer not only allows to reinforce LDPE at elevated temperatures but also functions as an electrical conductivity-reducing additive, which makes such thermoplastic ternary formulations possible candidates for the insulation of high-voltage power cables.

1 | INTRODUCTION

Power transmission technology plays an essential part in meeting the global demand for energy in a sustainable fashion. In particular, efficient high-voltage direct-current (HVDC) power cables are needed to reduce electrical losses during the transport of electricity over long distances of up to a few thousand kilometres [1]. HVDC cables allow the integration of renewable sources of energy, which are often harnessed far away from populated areas, into power grids.

The insulation material surrounding the conducting core of extruded undersea and underground HVDC cables is crucial for efficient long-distance power transmission. The electric field that an insulation material can withstand determines the transmission voltage and, hence, the electrical power that a

cable can transport. One essential requirement is that the insulation has a very low direct-current (DC) electrical conductivity σ_{DC}, which reduces leakage currents and Joule heating. It is, therefore, also important that the insulation is able to dissipate heat to prevent the formation of hot spots, which heighten the risk of thermal runaway and cable breakdown [1]. In addition to possessing a very low σ_{DC} and a high thermal conductivity κ to transport heat away from the core of the cable, the insulation material must also display a high degree of thermomechanical stability. The typical operating temperature of an HVDC power cable ranges from 70 to 90°C, but higher temperatures can be reached during emergency conditions such as power surges and lightning strikes [2]. At these elevated temperatures, the insulation material must maintain dimensional stability.

The most common insulation material for extruded HVDC cables is crosslinked polyethylene (XLPE), which is produced from low-density polyethylene (LDPE). LDPE has favourable flow properties for melt extrusion and can be produced with a high degree of chemical and physical cleanliness, which is advantageous for attaining a very low σ_{DC}. However, its thermomechanical properties are inadequate due to its low melting temperature $T_m^{LDPE} \sim 110°C$. Conventionally, this shortcoming is circumvented by crosslinking LDPE with peroxides, which, however, releases by-products that can increase σ_{DC} unless they are removed through a degassing step [3, 4].

An alternative type of insulation material that currently receives considerable interest comprises thermoplastic blends that incorporate polypropylene (PP) or polypropylene copolymers [5–13]. These thermoplastic materials can be used without crosslinking due to their high melting temperature $T_m^{PP} \sim 170°C$ in case of isotactic PP. Furthermore, PP grades such as those used for capacitor and supercapacitor applications are known to possess a very low electrical conductivity [14]. One disadvantage of isotactic PP is its stiffness and low-temperature brittleness due to its high glass transition temperature $T_g \sim 0°C$. Therefore, syndiotactic PP [10, 15, 16], PP copolymers [9–11], as well as blends that comprise PP or PP copolymers [5, 6, 8, 17–22] have been studied as potential materials for high-voltage cable insulation. These include blends of isotactic PP and various polyethylenes [20–22]. For instance, Dabbak et al. investigated the alternating-current (AC) breakdown strength of various isotactic PP:LDPE and PP:high-density polyethylene (HDPE) blends and observed that blends feature a dielectric strength between those of PP and polyethylene, with PP yielding the lowest value [20]. Furthermore, we have recently studied blends of LDPE and PP, which display a considerable increase in storage modulus in the temperature window $T_m^{LDPE} < T < T_m^{PP}$ provided that the PP phase is continuous, only achieved with a PP content of more than 40 weight percent (wt%) [22]. To alleviate the immiscibility of LDPE and PP, we added a linear triblock copolymer polystyrene-*b*-(ethylene-*co*-butylene)-*b*-polystyrene (SEBS), which has been used as a compatibiliser for a wide range of polymer blends [23–29] including blends of PP and polyethylene [25, 30]. We found that the addition of 10 wt% SEBS to PP:LDPE blends, which do not display a continuous PP phase, allowed to increase both the storage modulus and the creep resistance above T_m^{LDPE}. We assigned the improvement in creep resistance to modification of the interface between PP domains and the surrounding LDPE matrix [22].

Here, we investigate the impact of the PP content on the thermomechanical properties as well as σ_{DC} and κ of SEBS:PP:LDPE ternary blends. We find that the addition of only 5 wt% SEBS widens the composition range for which the blends demonstrate a higher stiffness above T_m^{LDPE}. Importantly, the addition of SEBS considerably improves the reproducibility of the observed thermomechanical properties, that is, the behaviour of SEBS:PP:LDPE ternary blends becomes more robust with regard to slight changes in processing conditions. Further, we observe that both σ_{DC} and κ decrease with PP content, meaning that there is an optimal blend composition

where adequate thermomechanical and electrical properties are achieved without unduly compromising the heat transport through the material.

2 | RESULTS AND DISCUSSION

2.1 | Choice of materials and compounding temperature

The PP grade that is used in this study displays a $T_m^{PP} \sim 170°C$ (see Figure 1a), which means that compounding must be
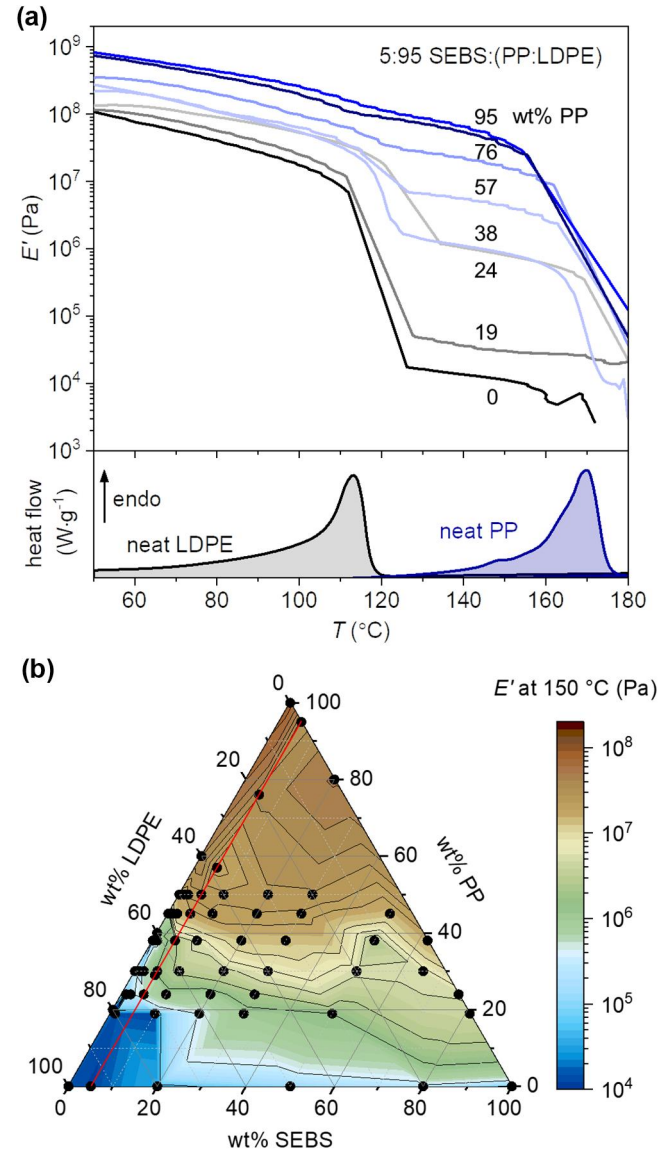
FIGURE 1 (a) Top: storage modulus E' measured with dynamic mechanical analysis (DMA) as a function of the temperature for different PP contents ranging from 0 (black) to 95 wt% (navy); bottom: differential scanning calorimetry (DSC) first heating thermograms of neat LDPE (black) and neat PP (navy); (b) storage modulus E' at 150°C of the ternary system SEBS:PP:LDPE; red line corresponds to blend compositions with 5 wt% SEBS. The DSC thermograms of neat LDPE and neat PP are reproduced from Reference [16]

carried out at a temperature of at least 180°C. We chose to work with a SEBS grade that remains ordered at 180°C, motivated by the work of Veenstra et al. who studied how the order-disorder transition (ODT) of SEBS influences the blend microstructures that can be obtained [31]. Specifically, Veenstra et al. observed that compounding of SEBS:PP blends below the ODT temperature of SEBS, where the block copolymer evolves from a phase-separated to a single-phase state, allows to obtain stable co-continuous blend microstructures over a wide range of compositions. We carried out oscillatory shear rheometry and variable-temperature small-angle X-ray scattering (SAXS) to confirm that the SEBS grade, which we had selected for our study, remains ordered up to 240°C (Figures S1 and S2). The crossover temperature between the storage and loss moduli of neat SEBS occurs at ~240°C (Figure S1) and SAXS diffractograms indicate that the SEBS grade features cylindrical domains from room temperature up to 240°C (Figure S2), which suggests that the copolymer remains ordered at 180°C. Hence, compounding was done at 180°C using a micro-compounder, which produced 2.5 g batches of different formulations (see Experimental for details as well as section on upscaling where we instead used a larger extruder line). We chose to carry out compounding in one step, that is, SEBS, PP and LDPE were added at the same time, because differential scanning calorimetry (DSC) thermograms indicate that the three components are mutually immiscible, as evidenced by a close to invariant T_m^{LDPE} and T_m^{PP} for all studied compositions (Figure S3).

## 2.2 | Thermomechanical properties of SEBS:PP:LDPE

Dynamic mechanical analysis (DMA) was used to study the thermomechanical behaviour of SEBS:PP:LDPE ternary blends across a wide temperature range. The storage modulus E' was obtained from DMA heating thermograms recorded at a maximum strain of 1%, which lies at the edge of the linear viscoelastic region at 150°C (Figure S4; see Figure S5 of tensile deformation of the blend components and selected ternary blends at room temperature). A plot of the storage modulus E' at 150°C, which lies in the temperature window $T_m^{LDPE} < T < T_m^{PP}$ (Figure 1a), reveals that the presence of SEBS reduces the amount of PP that is needed to considerably stiffen the material (Figure 1b). In case of PP:LDPE binary blends, a PP content of at least 40 wt% is needed to significantly increase the storage modulus at 150°C compared to $E' \sim 10^4$ Pa of neat LDPE. The addition of as little as 2 wt% SEBS to PP:LDPE results in ternary blends that display a higher storage modulus even at significantly lower PP contents. In addition, we observe that at 50°C, ternary blends, which contain at least 60 wt% LDPE and less than 10 to 20 wt% SEBS, feature a stiffness similar to that of neat LDPE, that is, $E' \sim 200$ MPa (Figure S4), meaning that the material will display an adequate degree of flexibility. Interestingly, ternary blends with an appropriate composition (e.g. 20:38:42 SEBS:PP:LDPE studied in the section on

upscaling) display both an increase in E' at $T_m^{LDPE} < T < T_m^{PP}$ compared to LDPE, SEBS:LDPE and SEBS:PP as well as a lower E' at lower temperatures, for example, 50°C, compared to PP.

2.3 | Influence of 5 wt% SEBS on the thermomechanical properties

In further experiments, we chose to concentrate on ternary blends that contain 5 wt% SEBS. To quantify the effect of SEBS on the storage modulus, we compared the storage moduli of PP:LDPE binary blends and 5:95 SEBS:(PP:LDPE) ternary blends at 150°C (Figure 2). In case of PP:LDPE binary blends, the storage modulus increases from about 10^4 Pa below 40 wt% PP to more than 10^7 Pa above this composition threshold, which we explain with the emergence of a continuous PP phase. The SEBS-containing ternary blends on the other hand show a substantial increase in storage modulus already at a lower PP content. In our previous work, we have observed that SEBS assembles both at the interface between PP and LDPE domains as well as within PP domains and assigned the improved thermomechanical properties for compositions where PP not yet forms a continuous phase to the modified PP:LDPE interface [22]. For example, for a composition of 24 wt% PP, we observe a storage modulus of close to 10^6 Pa in case of the ternary blend, whereas for the binary blend with 25 wt% PP, a much lower value of about 10^4 Pa is observed. In contrast, blends with more than 40 wt% PP, where the PP phase is continuous (see discussion below), exhibited a slight reduction in storage modulus when 5 wt% SEBS was added.

For the blends containing PP and LDPE in a ratio of 25:75, which lies below the percolation threshold of PP
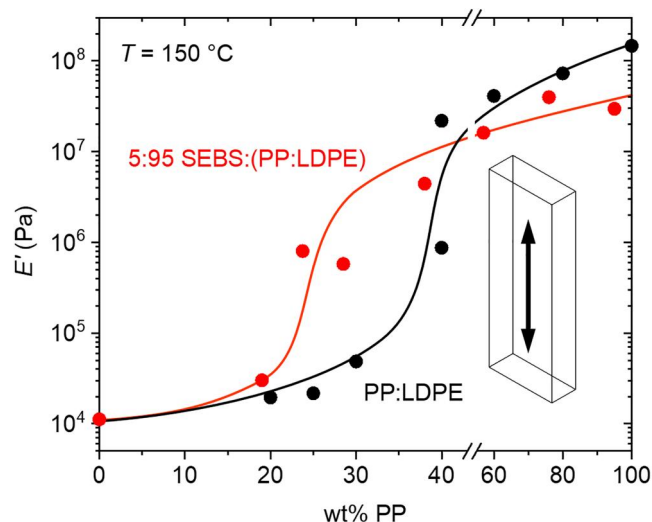

FIGURE 2 Storage modulus measured at 150°C with DMA as a function of PP content of LDPE, PP, the binary blends of LDPE and PP (black circles), and the corresponding materials with 5 wt% SEBS (red circles); solid lines are a guide to the eye. The storage moduli of PP:LDPE binary blends are obtained from Reference [16]

domains, the addition of 5 wt% SEBS significantly increases the storage modulus above T_m^{LDPE} (Figure 3a). At 150°C, the 5:95 SEBS:(PP:LDPE)$_{25:75}$ ternary blend displays a median $E' \sim 4 \times 10^5$ Pa, which is one order of magnitude higher than the median value of $E' \sim 4 \times 10^4$ Pa observed for the 25:75 PP:LDPE binary blend. The storage modulus measured at 150°C for different samples (prepared by varying the compounding time) displays a larger spread in case of binary as compared to ternary blends (Figure 3a; see Figure S5 for multiple DMA thermograms of neat LDPE). Evidently, the addition of SEBS reduces the effect of slight changes in processing conditions (i.e. the compounding time) on the thermomechanical properties. SEM micrographs of cryo-fractured sample surfaces indicate that the addition of SEBS results in dark and bright subdomains in the non-LDPE regions, which correspond to SEBS and PP, respectively (Figure 3b and Figure S8). Furthermore, the SEM images indicate a similar number of SEBS:PP domains in case of the 5:95 SEBS:(PP:LDPE)$_{25:75}$ ternary blend compared to PP domains in the 25:75 PP:LDPE binary blend.

We also compared the storage modulus of blends with a higher PP content, that is, blends containing 40:60 PP:LDPE, with and without 5 wt% SEBS (Figure 4a). In the absence of SEBS, the 40:60 PP:LDPE binary blend displays a median storage modulus at 150°C of 3×10^6 Pa, which increases to $E' \sim 5 \cdot 10^6$ Pa upon the addition of SEBS. However, if we compare the mean storage modulus at 150°C, both the binary and ternary blends (prepared with varying compounding times) show similar values of $E' \sim 6 \times 10^6$ Pa. This is due to the very large spread in values for the binary blend compared to the ternary blends. SEM images indicate that for blends based on 40:60 PP:LDPE, the PP and LDPE domains start to be co-continuous (Figure 4b). The addition of 5 wt% SEBS, however, does not appear to change the size of domains. Being at the onset of phase inversion at this blend composition, it is unsurprising that the compounding time has a distinct impact on the degree of continuity of the PP domains in case of the binary blend. In contrast, the microstructure of ternary blends appears to be more robust with regard to changes in processing conditions (Figure S9).

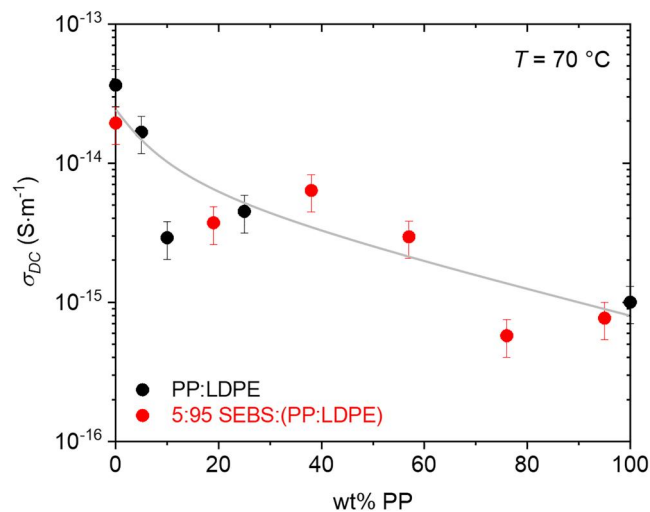## 2.4 | DC electrical conductivity

An insulation material must also exhibit a very low DC electrical conductivity. Hence, we investigated the effect of PP composition on σ_{DC} of the PP:LDPE binary blends and the 5:95 SEBS:(PP:LDPE) ternary blends. The addition of 5 wt% SEBS does not have a significant effect on σ_{DC}, but incorporating PP lowers σ_{DC}, which we attribute to the inherently low $\sigma_{DC} \sim 1 \times 10^{-15}$ S·m^{-1} of the capacitor-grade PP used for this study (Figure 5). The addition of 10 wt% PP strongly reduces the electrical conductivity from $\sigma_{DC} \sim 36 \times 10^{-15}$ S·m^{-1} for neat LDPE to $3 \cdot 10^{-15}$ S·m^{-1} for the 10:90 PP:LDPE binary blend, calculated from charging currents measured after 46 h at an electric field of 30 kV·mm^{-1} at 70°C. For a ternary
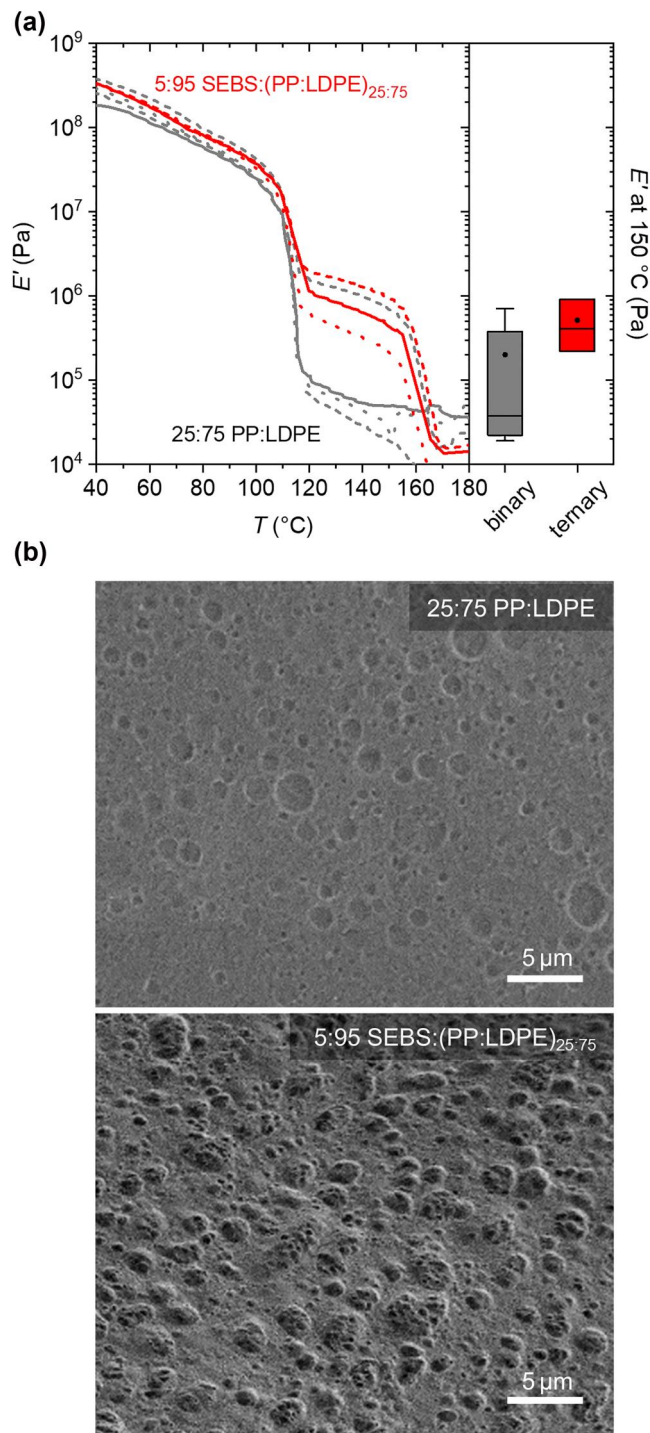
FIGURE 3 (a) Storage modulus E' measured with a DMA as a function of the temperature of the 25:75 PP:LDPE binary blends (grey) and the corresponding 5:95 SEBS:(PP:LDPE)$_{25:75}$ ternary blends (red). Solid, dashed and dotted lines correspond to compounding times of five (solid lines), 10 (dashed lines), and 15 min (dotted lines), respectively (left); and box plots of E' at 150°C of the 25:75 PP:LDPE binary blends (grey) and the corresponding 5:95 SEBS:(PP:LDPE)$_{25:75}$ ternary blends (red) at different compounding times, where the box corresponds to the interquartile range, the line in each box reflects the median, the filled circle corresponds to the mean, and the whiskers show the 1.5 interquartile range (right); (b) SEM micrographs of the cryofractured and etched surfaces of the 25:75 PP:LDPE binary blend (top) and the 5:95 SEBS:(PP:LDPE)$_{25:75}$ ternary blend (bottom) after compounding for 5 min
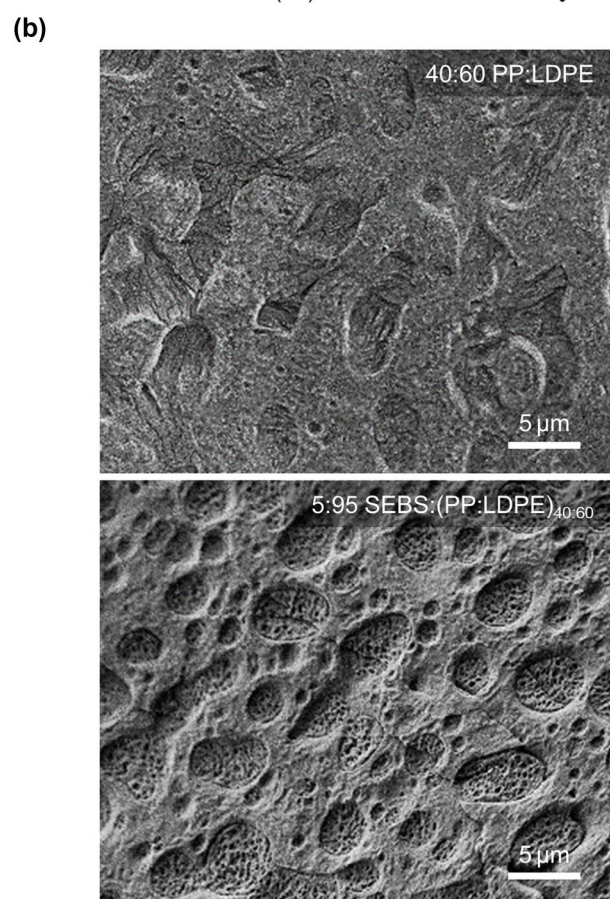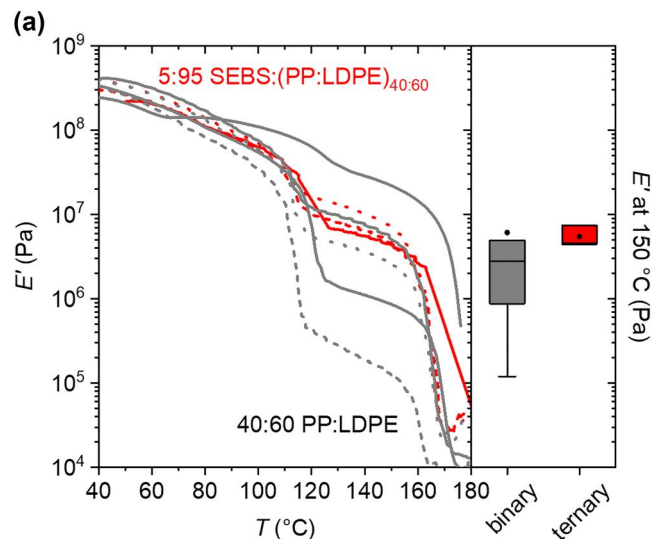
FIGURE 4 (a) Storage modulus E' measured with a DMA as a function of temperature of 40:60 PP:LDPE binary blends (grey) and the corresponding 5:95 SEBS:(PP:LDPE)$_{40:60}$ ternary blends (red). Solid, dashed and dotted lines correspond to compounding times of five (solid lines), 10 (dashed lines), and 15 min (dotted lines), respectively (left), and box plots of E' at 150°C of the 40:60 PP:LDPE binary blends (grey) and the corresponding 5:95 SEBS:(PP:LDPE)$_{40:60}$ ternary blends (red) at different compounding times, where the box corresponds to the interquartile range, the line in each box reflects the median, the filled circle represents the mean, and the whiskers show the 1.5 interquartile range (right); (b) SEM micrographs of the cryofracture surfaces of the 40:60 PP: LDPE binary blend (top) and the 5:95 SEBS:(PP:LDPE)$_{40:60}$ ternary blend (bottom) after compounding for 5 min

FIGURE 5 DC electrical conductivity σ_{DC} at 70°C and 30 kV·mm^{-1} after 46 h of LDPE, PP, PP:LDPE binary blends of increasing PP content (black) and the corresponding materials with 5 wt% SEBS (red), plotted as a function of PP content. All reported values are obtained from single measurements apart from σ_{DC} of the 5:95 SEBS:(PP:LDPE)$_{40:60}$ ternary blend (i.e. 38 wt% PP), which is the mean of 5 measurements; the estimated percentage error of 30% for σ_{DC} is based on the standard deviation of these five samples (Figure S10)
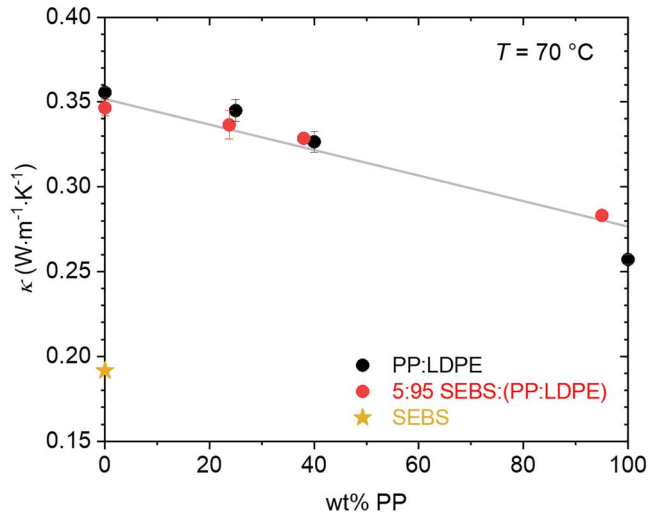
blend containing 19% PP, we measured a similar value of $\sigma_{DC} \sim 4\times10^{-15}$ S·m^{-1}. A higher amount of PP only resulted in a slight further reduction in σ_{DC}. Hence, percolation of PP domains above 40 wt% PP, inferred from SEM, is not responsible for the observed decrease in σ_{DC}. Evidently, PP can be considered as a conductivity-reducing additive for LDPE, similar to, for instance, HDPE [32] and metal oxide nanoparticles [33–36].
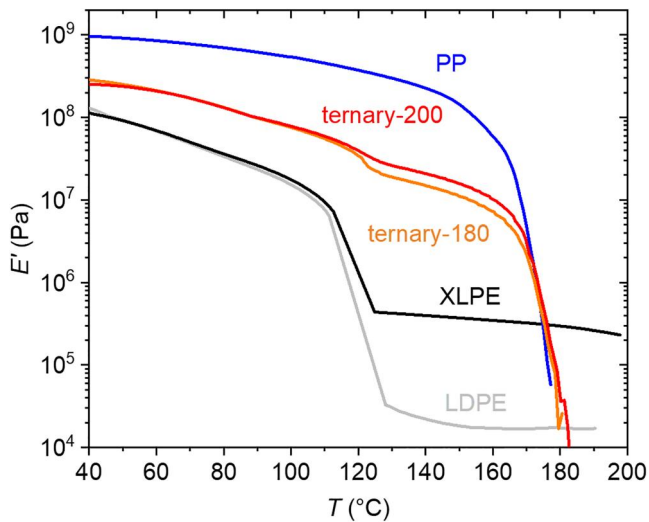
2.5 | Thermal conductivity

We also characterised the thermal conductivity of selected binary and ternary blends. At 70°C, the incorporation of 5 wt% SEBS does not have any considerable influence on κ despite the considerably lower value of 0.19 W·m^{-1}·K^{-1} for neat SEBS. However, we do observe a linear decrease in κ with PP content (Figure 6). The reduction in κ with increasing amount of PP can be attributed to the fact that at 70°C neat PP has a thermal conductivity of 0.26 W·m^{-1}·K^{-1}, which is substantially lower than the value of 0.36 W·m^{-1}·K^{-1} measured for neat LDPE. The relationship between κ and PP content is not affected by the percolation of PP around 40 wt% but follows the rule of mixtures (Figure S11b). The same behaviour is also observed at room temperature (Figure S11a) and at 90°C (Figure S11c). We also note that the thermal conductivity of neat PP increased upon the addition of 5 wt% SEBS (i.e. 5:95 SEBS:PP; see Figure 6 and Figure S12), which we tentatively explain with a change in PP microstructure. We conclude that in terms of thermal conductivity, the formulations studied show that the incorporation of less PP is favourable for cable applications.

2.6 | Upscaling of one promising ternary blend formulation

The formulations discussed up to now were compounded with a twin-screw micro-compounder in batches of about 2.5 g. To investigate if SEBS:PP:LDPE ternary blends can also be processed with a larger extrusion line, we compounded a formulation containing 20 wt% SEBS, 38 wt% PP and 42 wt% LDPE using a twin screw extruder that operated with a throughput rate of about 6 kgh^{-1}. We selected this formulation with help of Figure 1b and

Figure S4, which suggest that for this composition, a material can be expected that shows significantly higher stiffness than LDPE at $T_m^{LDPE} < T < T_m^{PP}$ while retaining higher flexibility compared to PP at lower temperatures. DMA thermograms indicate that the upscaled ternary blend is significantly stiffer at elevated temperatures than LDPE and XLPE as evidenced by a storage modulus of $E' \sim 1\times10^7$ Pa at 150°C (Figure 7). At the same time, this material exhibits a substantially reduced $E' \sim 2\times10^8$ Pa at 50°C compared to neat PP with $E' \sim 9\times10^8$ Pa (Figure 7). Further, the upscaled ternary blend features promising dielectric properties as evidenced by a low $\sigma_{DC} \sim 2\times10^{-15}$ S·m^{-1} at 70°C and 30 kV·mm^{-1}, which is comparable to the value measured for neat PP (Figure 8a).
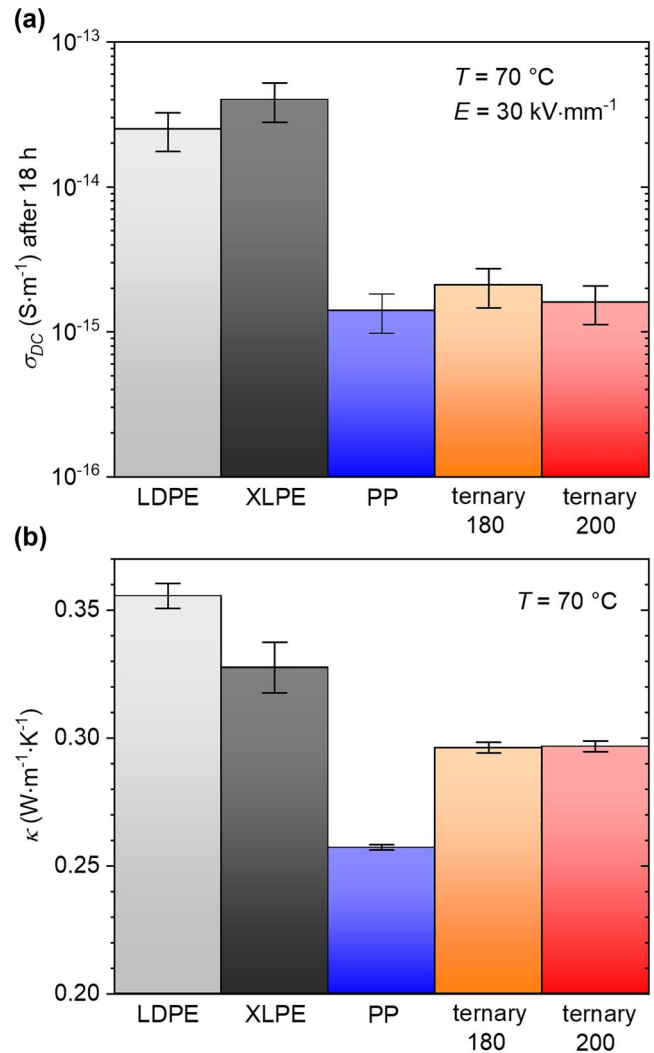

FIGURE 6 Mean thermal conductivity κ at 70°C plotted as a function of PP content, low-density polyethylene (LDPE), PP, PP:LDPE binary blends (black), the corresponding materials with 5 wt% SEBS (red), and neat SEBS (yellow star); grey solid line drawn to guide the eye

FIGURE 7 Storage modulus E' measured with dynamic mechanical analysis as a function of the temperature of LDPE (grey), XLPE (black), PP (blue), and the upscaled 20:38:42 SEBS:PP:LDPE ternary blend compounded at 180°C (orange) and 200°C (red)

FIGURE 8 (a) σ_{DC} obtained after 18 h at 70°C and an electric field of 30 kV·mm^{-1} (a percentage error of 30% is based on a comparison of five samples of the 5:95 SEBS:(PP:LDPE)$_{40:60}$ ternary blend; see Figure S10), and (b) κ at 70°C (error bars are based on the standard deviation calculated from five measurements of each sample), of LDPE (grey), XLPE (black), PP (blue), and the upscaled 20:38:42 SEBS:PP:LDPE ternary blend compounded at 180°C (orange) and 200°C (red)

The ternary blend has a thermal conductivity of $\kappa \sim 0.30$ W·m^{-1}·K^{-1} at 70°C, which lies in between the values measured for XLPE and PP (Figure 8b). Excitingly, E', σ_{DC} and κ of the upscaled formulation are comparable when increasing the compounding temperature from 180 to 200°C, which confirms that the properties of SEBS:PP:LDPE ternary blends are not overly affected by changes in processing conditions.

3 | CONCLUSIONS

The addition of 5 wt% SEBS to PP:LDPE blends improves the thermomechanical properties for LDPE-rich compositions where PP domains do not percolate. As a result, a wider range of PP compositions can be considered for the design of materials with the potential to be used as HVDC cable insulation. Furthermore, the incorporation of 5 wt% SEBS increases the robustness of ternary blends towards slight changes in processing conditions. The DC electrical and thermal conductivity change significantly with PP content while the presence of a small amount of SEBS has no noticeable effect. We conclude that LDPE-rich ternary blends with a content of 24 to 40 wt% PP display the best combination of properties in terms of an increase in storage modulus above the melting temperature of LDPE and a reduction in electrical conductivity while not unduly reducing the thermal conductivity. Certainly, the use of SEBS as an additive for PP:LDPE blends increases the range of suitable compositions and, hence, may assist with the development of thermoplastic insulation materials for HVDC power cables. It would, therefore, be of great interest to investigate the dielectric properties in more detail, including further measurements of the DC electrical conductivity but also space charge accumulation and breakdown strength, both of neat SEBS:PP:LDPE ternary blends as well as thermally aged material.

4 | ACKNOWLEDGEMENTS

5 | EXPERIMENTAL

Materials. LDPE with a MFI ~ 2 g/10 min (190°C/2.16 kg), $M_n \sim 13$ kg·mol^{-1}, PDI ~ 9 and number of long-chain branches ~ 1.9 per 1000 carbons was obtained from Borealis AB. Isotactic polypropylene with an $M_n \sim 40$ kg·mol^{-1}, $M_w \sim 348$ kg·mol^{-1}, PDI ~ 8.6 and isotacticity >90% was also obtained from Borealis AB. Polystyrene-*b*-(ethylene-*co*-butylene)-*b*-polystyrene (SEBS) with a MFI <1 g/10 min (230°C/2.16 kg) and 18.5%–22.5% polystyrene content was obtained from Kraton Corporation (Kraton G1642 HU).

Compounding and sample preparation. The binary and ternary blends were compounded for 5, 10 or 15 min at 180°C with an Xplore Micro Compounder MC5 at a screw speed of 50 r/min followed by extrusion, resulting in about 2.5 g of material, which was cut into pieces. For upscaling, compounding was done with a Coperion ZSK 26 K 10.6 twin screw extruder at 120 r/min and temperatures of 180 or 200°C, followed by extrusion and pelletisation. The throughput rate was approximately 6 kgh^{-1}. The extrudate was cut into pellets. Samples for all characterisation methods were cut from plates that had been melt-pressed at 200°C for ~ 1 min at a pressure of up to 4 MPa, resulting in 1.25 mm thick plates for DSC, DMA, SEM and WAXS, 0.3 mm for DC electrical conductivity measurements, 4.6 mm for thermal conductivity measurements and 0.1 mm for tensile testing.

Differential Scanning Calorimetry (DSC). DSC measurements were carried out under nitrogen between -50 and 200°C at a scan rate of 10°C min^{-1}, using a Mettler Toledo DSC2 calorimeter equipped with an HSS7 sensor and a TC-125 MT intercooler. The sample weight was 5–10 mg.

Scanning Electron Microscopy (SEM). Samples for SEM were cryofractured and subsequently etched for 45 min using a solution of 1 wt% potassium permanganate in a mixture of sulphuric acid, *ortho*-phosphoric acid and water, followed by cleaning in hydrogen peroxide, water and methanol. The etched surfaces were sputtered with palladium and imaged with a LEO Ultra 55 SEM instrument, using an acceleration voltage of 3 kV.

Small angle X-ray scattering (SAXS). Transmission SAXS diffractograms were obtained using a Mat:Nordic instrument from SAXLAB equipped with a Rigaku 003+ high brilliance micro-focus Cu-radiation source (wavelength = 1.5406 Å) and a Pilatus 300K detector placed at a distance of 1072 mm from the sample. The sample was heated with a Linkam stage and SAXS diffractograms were obtained during heating at room temperature and at 100–240°C with temperature steps of 20°C.

Rheometry. Oscillatory shear rheology was carried out with a DHR-3 instrument from TA instruments equipped with an environmental test chamber. The geometry used was a parallel plate with a diameter of 25 mm. For the temperature sweep experiment, the frequency and maximum strain were set to 1 Hz and 0.5%, respectively. The strain sweep experiment with neat PP and the 5:95 SEBS:(PP:LDPE)$_{25:75}$ ternary blend was conducted at 150°C and a frequency of 1 Hz.

Dynamic mechanical analysis (DMA). DMA was carried out using a TA Q800 DMA in tensile mode on 20×5 mm pieces cut from 1.25mm-thick melt-pressed films. Variable-temperature measurements were done at a heating rate 2°C min^{-1}, with a maximum strain of 1% and a frequency of 0.5 Hz.

Tensile testing. Tensile testing was done with an Instron 5565A with a gauge length of 20 mm at a crosshead speed of 50 mm·min^{-1}.

DC conductivity measurements. The test cell consisted of a three-electrode system setup (measuring area of $\emptyset = 60$ mm), placed in an oven at 70°C and connected to a high-voltage power supply (Glassman FJ40P03). A DC voltage of 9.9 kV was applied across 0.33-mm-thick specimen films for 23 h and the voltage was switched off for 1 h. The same voltage was subsequently re-applied for another 23 h. The DC electrical conductivity was calculated based on the charging currents obtained at the end of each 23 h period. The volume leakage current was recorded with a Keithley 6517B electrometer and dynamically averaged. In addition, a low-pass filter was added into the circuit at the high-voltage side for limiting the current in case of specimen breakdown and for filtering out high-frequency noise.

Thermal conductivity measurements. The thermal conductivity was measured with a TPS 2500 S instrument from Hot Disk, which uses a transiently heated plane sensor to simultaneously heat and measure temperature. The 7577 Kapton sensor was sandwiched between two 4.6-mm-thick specimen films with a diameter of 34 mm, fixed between two steel blocks. The set-up was placed in an oven heated to 70 or 90°C. During each measurement, 20 mW of heating power was supplied over 5 s, resulting in a probing depth of ∼2 mm.

CONFLICT OF INTEREST
None.

DATA AVAILABILITY STATEMENT
Data available on request from the authors.

ORCID
Amir Masoud Pourrahimi https://orcid.org/0000-0001-5867-0531
Christian Müller https://orcid.org/0000-0001-7859-7909

REFERENCES
1. Montanari, G.C., et al.: Criteria influencing the selection and design of HV and UHV DC cables in new network applications. High Volt. 3(2), 90–95 (2018)
2. Mazzanti, G., Marzinotto, M.: Extruded Cables for High-Voltage Direct-Current Transmission. Wiley, NJ (2013)
3. Smedberg, A., Hjertberg, T., Gustafsson, B.: Crosslinking reactions in an unsaturated LDPE. Polymer. 38(16), 4127–4138 (1997)
4. Sahyoun, J., et al.: Diffusion mechanism of byproducts resulting from the peroxide crosslinking of polyethylene. J. Appl. Polym. Sci. 134(9), 44525 (2017)
5. Zhou, Y., et al.: Evaluation of polypropylene/polyolefin elastomer blends for potential recyclable HVDC cable insulation applications. IEEE Trans. Dielectr. Electr. Insul. 22(2), 673–681 (2015)
6. Hosier, I.L., Vaughan, A.S., Swingler, S.G.: An investigation of the potential of polypropylene and its blends for use in recyclable high voltage cable insulation systems. J. Mater. Sci. 46(11), 4058–4070 (2011)
7. Diao, J., et al.: Thermoplastic isotactic polypropylene/ethylene-octene polyolefin copolymer nanocomposite for recyclable HVDC cable insulation. IEEE Trans. Dielectr. Electr. Insul. 24(3), 1416–1429 (2017)
8. Green, C.D., et al.: Thermoplastic cable insulation comprising a blend of isotactic polypropylene and a propylene-ethylene copolymer. IEEE Trans. Dielectr. Electr. Insul. 22(2), 639–648 (2015)
9. Hosier, I.L., et al.: Propylene based systems for high voltage cable insulation applications. J. Phys.: Conf. Ser. 183, 012015 (2009)
10. Hosier, I.L., et al.: Morphology, thermal, mechanical and electrical properties of propylene-based materials for cable applications. Conference Record IEEE International Symposium on Electrical Insulation, pp. 502–505. Canada, Vancouver (2010)
11. Huang, X., et al.: Polypropylene based thermoplastic polymers for potential recyclable HVDC cable insulation applications. IEEE Trans. Dielectr. Electr. Insul. 24(3), 1446–1456 (2017)
12. Zhang, C., et al.: Space charge behaviors of low-density polyethylene blended with polypropylene copolymer. Polymer. 43(8), 2261–2266 (2002)
13. Zhang, C., et al.: Morphology and electrical breakdown properties of LDPE-polypropylene copolymer blends. J. Polym. Sci., Part B: Polym. Phys 39(15), 1741–1748 (2001)
14. Andritsch, T., Vaughan, A., Stevens, G.C.: Novel insulation materials for high voltage cable systems. IEEE Electr. Insul. Mag. 33(4), 27–33 (2017)
15. Kim, D.W., et al.: Influence of morphology on electrical properties of syndiotactic polypropylene compared with those of isotactic polypropylene. Jpn. J. Appl. Phys. 38, 3580–3584 (1999)
16. Setz, S., et al.: Morphology and mechanical properties of blends of isotactic or syndiotactic polypropylene with SEBS block copolymers. J. Appl. Polym. Sci. 59(7), 1117–1128 (1996)
17. Hong, S.K., et al.: Polypropylene-based soft ternary blends for power cable insulation at low-to-high temperature. J. Appl. Polym. Sci. 139, 51619 (2021)
18. Huang, X., et al.: Material progress toward recyclable insulation of power cables part 2: polypropylene-based thermoplastic materials. IEEE Electr. Insul. Mag. 36(1), 8–18 (2020)
19. Yu, S., et al.: Insulative ethylene-propylene copolymer-nanostructured polypropylene for high-voltage cable insulation applications. Polymer. 202, 122674 (2020)
20. Dabbak, S.Z.A., et al.: Electrical properties of polyethylene/polypropylene compounds for high-voltage insulation. Energies. 11(6), 1448 (2018)
21. Ouyang, Y., et al.: Recyclable polyethylene insulation via reactive compounding with a maleic anhydride-grafted polypropylene. ACS Appl. Polym. Mater. 2(6), 2389–2396 (2020)
22. Ouyang, Y., et al.: High-temperature creep resistant ternary blends based on polyethylene and polypropylene for thermoplastic power cable insulation. J. Polym. Sci. 59(11), 1084–1094 (2021)
23. Nam, G.J., Kim, K.Y., Lee, J.W.: The effect of SEBS on interfacial tension and rheological properties of LDPE/PS blend. J. Appl. Polym. Sci. 96(3), 905–911 (2005)
24. Virgilio, N., et al.: Modified interfacial tensions measured in situ in ternary polymer blends demonstrating partial wetting. Polymer. 51(6), 1472–1484 (2010)
25. Gupta, A.K., Purwar, S.N.: Studies on binary and ternary blends of polypropylene with SEBS, PS, and HDPE. II. Tensile and impact properties. J. Appl. Polym. Sci. 30(5), 1799–1814 (1985)
26. Heino, M., et al.: Compatibilization of polyethylene terephthalate/polypropylene blends with styrene–ethylene/butylene–styrene (SEBS) block copolymers. J. Appl. Polym. Sci. 65(2), 241–249 (1997)
27. Srinivasan, K.R., Gupta, A.K.: Mechanical properties and morphology of PP/SEBS/PC blends. J. Appl. Polym. Sci. 53(1), 1–17 (1994)
28. Rek, V., et al.: Morphology and properties of SEBS block copolymer compatibilized PS/HDPE blends. J. Elastomers Plastics. 40(3), 237–251 (2008)
29. Bedjaoui, K., et al.: The effect of compatibilizer SEBS on the mechanical, morphological and thermal properties of the polystyrene/poly (styrene-co-acrylonitrile) copolymer blends. Mater. Res. Express. 6(10), 105334 (2019)
30. Flaris, V., Wasiak, A., Wenig, W.: The effect of compatibilizers on the morphology of isotactic polypropylene/linear low-density polyethylene blends. J. Mater. Sci. 28(6), 1685–1688 (1993)
31. Veenstra, H., et al.: Co-continuous morphologies in polymer blends with SEBS block copolymers. Polymer. 40(24), 6661–6672 (1999)
32. Andersson, M.G., et al.: Highly insulating polyethylene blends for high-voltage direct-current power cables. ACS Macro Lett. 6(2), 78–82 (2017)

33. Nilsson, F., et al.: Nanocomposites and polyethylene blends: two potentially synergistic strategies for HVDC insulation materials with ultra-low electrical conductivity. Comp. B: Eng. 204, 108498 (2021)

34. Pourrahimi, A.M., et al.: Polyethylene nanocomposites for the next generation of ultralow-transmission-loss HVDC cables: insulation containing moisture-resistant MgO nanoparticles. ACS Appl. Mater. Interfaces. 8(23), 14824–14835 (2016)

35. Pourrahimi, A.M., Olsson, R.T., Hedenqvist, M.S.: The role of interfaces in polyethylene/metal-oxide nanocomposites for ultrahigh-voltage insulating materials. Adv. Mater. 30(4), 1703624 (2018)

36. Pourrahimi, A.M., et al.: Highly efficient interfaces in nanocomposites based on polyethylene and ZnO nano/hierarchical particles: a novel approach toward ultralow electrical conductivity insulations. Adv. Mater. 28(39), 8651–8657 (2016)

SUPPORTING INFORMATION

Additional supporting information may be found in the online version of the article at the publisher's website.